

MYELOID NEOPLASIA

JAK2-V617F and interferon- α induce megakaryocyte-biased stem cells characterized by decreased long-term functionality

Tata Nageswara Rao,¹ Nils Hansen,¹ Jan Stetka,^{1,2} Damien Luque Paz,¹ Milena Kalmer,³ Julian Hilfiker,¹ Max Endeke,⁴ Nouraz Ahmed,⁴ Lucia Kubovcakova,¹ Margareta Rybarikova,¹ Hui Hao-Shen,¹ Florian Geier,^{1,5} Christian Beisel,⁴ Stefan Dirnhöfer,⁶ Timm Schroeder,⁴ Tim H. Brummendorf,³ Dominik Wolf,⁷ Steffen Koschmieder,³ and Radek C. Skoda¹

¹Department of Biomedicine, Experimental Hematology, University Hospital Basel–University of Basel, Basel, Switzerland; ²Department of Biology, Faculty of Medicine and Dentistry, Palacky University, Olomouc, Czech Republic; ³Department of Hematology, Oncology, Hemostaseology, and Stem Cell Transplantation, Faculty of Medicine, Rheinisch-Westfälische Technische Hochschul (RWTH) Aachen University, Aachen, Germany; ⁴Department of Biosystems Science and Engineering, Eidgenössische Technische Hochschule Zurich, Basel, Switzerland; ⁵Swiss Institute of Bioinformatics, Basel, Switzerland; ⁶Institute of Medical Genetics and Pathology, University Hospital Basel, Basel, Switzerland; and ⁷Internal Medicine V, Department of Hematology and Oncology, Medical University Innsbruck, Innsbruck, Austria

KEY POINTS

- Expression of mutant JAK2 increased the proportion of megakaryocyte-biased CD41^{hi} hematopoietic stem cells with lower long-term potential.
- IFN α further increased the proportion of CD41^{hi} HSCs and depleted JAK2-mutant HSCs in mice and patients with MPN.

We studied a subset of hematopoietic stem cells (HSCs) that are defined by elevated expression of CD41 (CD41^{hi}) and showed bias for differentiation toward megakaryocytes (Mks). Mouse models of myeloproliferative neoplasms (MPNs) expressing JAK2-V617F (VF) displayed increased frequencies and percentages of the CD41^{hi} vs CD41^{lo} HSCs compared with wild-type controls. An increase in CD41^{hi} HSCs that correlated with JAK2-V617F mutant allele burden was also found in bone marrow from patients with MPN. CD41^{hi} HSCs produced a higher number of Mk-colonies of HSCs in single-cell cultures in vitro, but showed reduced long-term reconstitution potential compared with CD41^{lo} HSCs in competitive transplantations in vivo. RNA expression profiling showed an upregulated cell cycle, *Myc*, and oxidative phosphorylation gene signatures in CD41^{hi} HSCs, whereas CD41^{lo} HSCs showed higher gene expression of interferon and the *JAK/STAT* and *TNF α /NF κ B* signaling pathways. Higher cell cycle activity and elevated levels of reactive oxygen species were confirmed in CD41^{hi} HSCs by flow cytometry. Expression of *Epcr*, a marker for quiescent HSCs inversely correlated with expression of CD41 in mice, but did not show such reciprocal expression pattern in patients with MPN. Treatment with interferon- α further increased the frequency and percentage of CD41^{hi} HSCs and reduced the number of JAK2-V617F⁺ HSCs in mice and patients with MPN. The shift toward the CD41^{hi} subset of HSCs by interferon- α provides a possible mechanism of how interferon- α preferentially targets the JAK2 mutant clone. (*Blood*. 2021;137(16):2139-2151)

Introduction

Several studies have identified subsets of stem cells in the pool of phenotypic long-term hematopoietic stem cells (HSCs) with an intrinsic megakaryocytic (Mk) bias and propensity to commit directly to the Mk lineage.¹⁻⁶ These subsets of HSCs have been defined primarily by functional readouts and increased expression of endogenous cell surface proteins (eg, high CD41 [CD41^{hi}] or high c-Kit).^{4,7,8} Alternatively, expression of a reporter construct (VWF-GFP) has been used to identify Mk-biased HSCs.² Among the known HSC marker genes, increased expression of the endothelial protein C receptor (*Epcr*, encoded by the *Procr1* gene) on HSCs has been shown to mark functional long-term repopulating HSCs in mice.^{9,10}

Myeloproliferative neoplasms (MPNs) are clonal stem cell disorders caused by somatic gene mutations in *JAK2*, *CALR*, or *MPL*.¹¹ Patients with MPNs caused by mutated *JAK2* can have distinct phenotypic manifestations that are classified as polycythemia vera (PV) with significant expansion of erythropoiesis, essential thrombocythemia with increased production of megakaryocytes and platelets, or primary myelofibrosis (PMF) with extramedullary hematopoiesis in the spleen.¹² The concept of Mk lineage-biased subsets of HSCs provides a possible basis for the observation that the presence of the *JAK2*-V617F mutation in some patients with MPN can be restricted to 1 or 2 lineages (eg, granulocytes and/or platelets).^{13,14} In our previous studies in which we used transplantations of single HSCs, we observed that some recipient mice displayed a pure

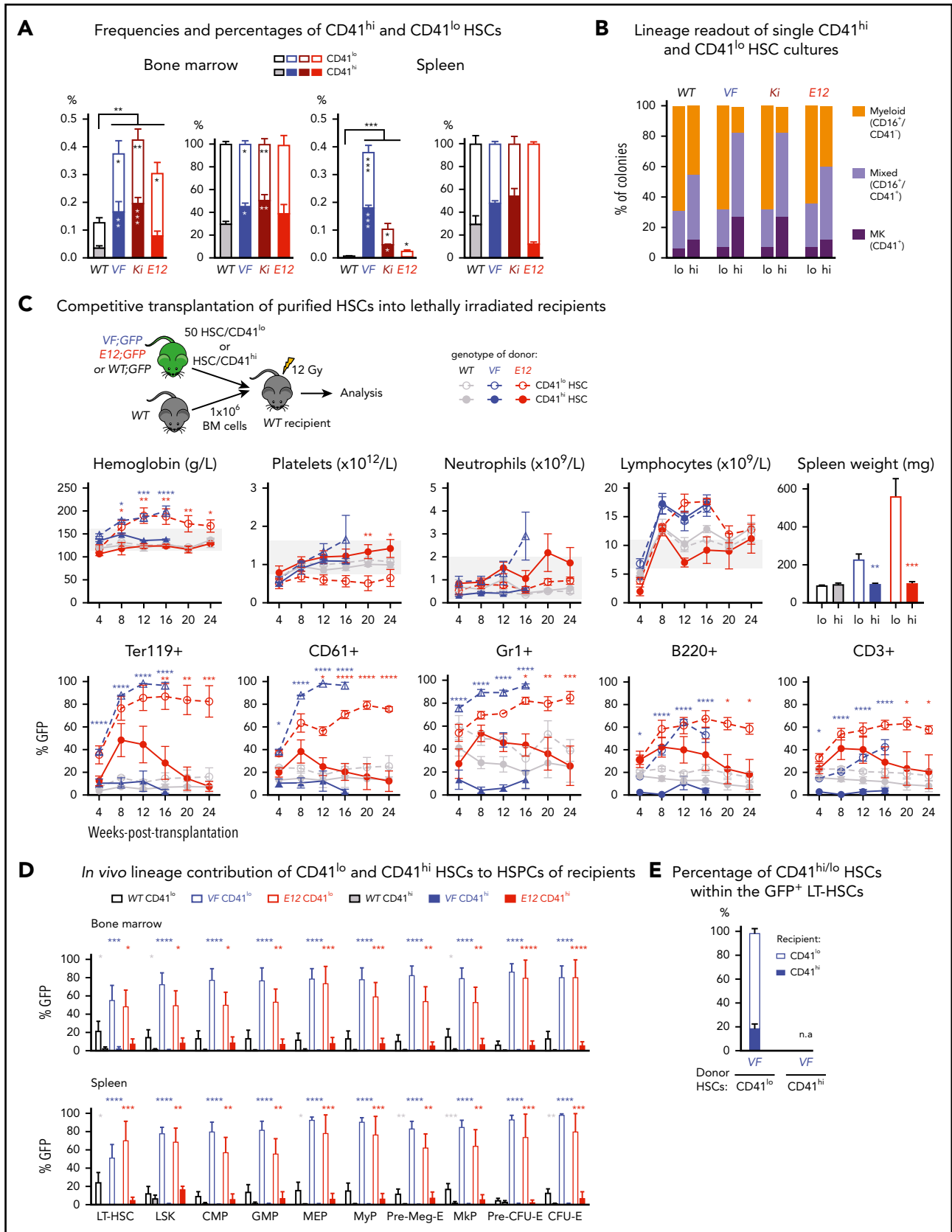


Figure 1. Increased frequency of CD41 expressing Mk-biased HSCs in mutant *JAK2*-expressing mice. (A) Frequencies (left) and percentages (right) of CD41^{hi} and CD41^{lo} HSCs within the phenotypic HSC compartment in BM in the indicated genotypes (n = 7 mice per genotype). Frequencies (left) and percentages (right) of CD41^{hi} and CD41^{lo} HSCs in the phenotypic HSC compartment in the spleen of the indicated genotype (n = 7 mice per genotype). (B) Analysis of colonies grown from a FACS-sorted single CD41^{hi} or CD41^{lo} HSC in liquid culture showing the percentages of colonies containing Mk (CD41⁺), myeloid (CD16⁺), or mixed (Mk and myeloid, CD41⁺/CD16⁺) cells after 10 days

thrombocytosis phenotype, whereas others displayed pure erythrocytosis, which appeared to be mutually exclusive.¹⁵ Interferon- α (IFN- α) is currently the only treatment, apart from stem cell transplantation, that can induce deep molecular remission in a subset of patients with MPNs.¹⁶ The mechanism of how IFN elicits these beneficial effects in MPN remains poorly understood. IFN- α was shown to promote cell cycle entry and increase the division rate of normal HSCs.¹⁷

In this study, we investigated the functional role of Mk-biased HSCs in MPN in mouse models and samples from patients with MPN. We also examined the responsiveness of HSCs that express mutant JAK2 toward IFN- α . We found that mutant JAK2 led to the expansion of a CD41^{hi} subset of HSCs and these CD41^{hi} HSCs were inferior to the CD41^{lo} subset of HSCs in sustaining long-term multilineage engraftment. Prolonged treatment with IFN- α further increased the proportion of CD41^{hi} HSCs in JAK2 mutant mice and patients with MPN and resulted in a reduction of quiescent CD41^{lo} HSCs capable of long-term maintenance of MPN, thus providing a possible mechanism of how IFN- α may induce molecular remissions in MPN.

Materials and methods

Mice

Tamoxifen inducible *SclCre;JAK2-V617F (VF)*, *SclCre;mJak2-V617F* knock-in (*Ki*), and *SclCre;JAK2 Exon12 (E12)* transgenic mice have been described.¹⁸⁻²⁰ JAK2 mutant mice were crossed with the *UBC-GFP* strain,²¹ and bone marrow (BM) cells that coexpress green fluorescent protein (GFP) as a reporter were used for competitive transplantations. *SclCre;JAK2-V617F/Ifr1^{-/-}* mice were generated by breeding *SclCre;JAK2-V617F* transgenic mice with the mice lacking *Ifr1*.²² Cre recombinase expression was induced by intraperitoneal injection of 2 mg tamoxifen (Sigma-Aldrich) for 5 consecutive days. All mice were of pure C57BL/6N background and were maintained in specific-pathogen-free conditions and in accordance with Swiss federal regulations.

plpC, pegIFN- α , and thrombopoietin treatment

Polyinosinic polycytidylic acid (plpC; P1530; Sigma-Aldrich) was injected intraperitoneally (300 μ g per mouse) every third day, and pegIFN- α (50 μ g per mouse) was injected subcutaneously once per week. For thrombopoietin (TPO) treatment, a single dose of recombinant mouse TPO (Peprotech) was injected intraperitoneally (200 μ g/kg per mouse).

BM transplantations

For competitive transplantation assays, fluorescence-activated cell sorting (FACS)-purified CD41^{hi} or CD41^{lo} HSCs subsets or Epcr^{hi} or Epcr^{lo} HSCs (50 cells) from *VF* or *E12* transgenic mice or wild-type (*WT*) mice coexpressing GFP were mixed with 1×10^6 BM cells of *WT* competitors and injected intravenously (in 200 μ L

phosphate buffered saline per mouse) into lethally irradiated (12 Gy) C57BL/6 recipients. Hematopoietic reconstitution was assessed by flow cytometry in peripheral blood (PB) at specified times.

Patients

The collection of blood and BM samples and clinical data from patients with MPN was approved by the Ethik Kommission Beider Basel and the ethics boards of the Universities of Innsbruck, Bonn, and RWTH Aachen. Written informed consent was obtained from all patients in accordance with the Declaration of Helsinki. The diagnosis of MPN was established according to the revised criteria of the World Health Organization.¹²

Results

Increased frequency of Mk-biased HSCs in mutant JAK2-expressing mice

We determined the frequencies of CD41^{hi} and CD41^{lo} HSCs in 3 Cre-inducible mouse models of MPN: transgenic mice expressing human JAK2-V617F (*VF*),¹⁸ a knock-in model expressing mouse *Jak2-V617F (Ki)*,¹⁹ and transgenic mice expressing human *JAK2-N542-E543del (E12)*.²⁰ The gating strategy for the CD41^{hi} subset of HSCs⁴ is shown in supplemental Figure 1A, available on the *Blood* Web site. As described previously,¹⁸⁻²⁰ the frequencies of HSCs in BM and spleen in all 3 JAK2 mutant strains were increased compared with *WT* controls (Figure 1A). *VF* and *Ki* mutant mice also showed an absolute and relative increase of CD41^{hi} HSCs in BM and spleen (Figure 1A), as well as an increase in CD41^{hi} hematopoietic progenitors (supplemental Figure 1B). This increase in CD41^{hi} HSCs was not observed in *E12* mutant mice.

To investigate whether CD41^{hi} HSCs also showed increased Mk differentiation potential, we performed single-cell liquid cultures of FACS-sorted CD41^{hi} or CD41^{lo} HSCs⁴ (Figure 1B; supplemental Figure 1C). The purity of the sorted HSCs was confirmed by postsort flow cytometry (supplemental Figure 1D). After 10 days of culture, CD41^{hi} HSCs generated a higher percentage of Mk colonies composed of larger CD41⁺ cells, whereas CD41^{lo} HSCs generated more myeloid or mixed-lineage colonies (Figure 1B; supplemental Figure 1E-F). This shift toward more Mk-biased output was less prominent in *WT* and *E12* mutant mice compared with *VF* and *Ki*.

To assess the lineage potential of CD41^{hi} and CD41^{lo} HSCs in vivo, we performed competitive transplantations of sorted HSCs into lethally irradiated recipient mice (Figure 1C). To monitor chimerism, we used donor mice that were crossed with *UBC-GFP* mice that express GFP in all blood lineages.²¹ Recipients of CD41^{lo} HSCs from *VF* and *E12* donors developed a PV phenotype with splenomegaly, whereas recipients of CD41^{hi}

Figure 1 (continued) of culture. We plated 48 single HSCs per mouse with 3 mice per genotype in 384-well plates (ie, a total of 144 single cells per genotype) and scored each well separately after 10 days of culture. (C) Setup of transplantations with purified CD41^{hi} and CD41^{lo} HSC subsets into lethally irradiated recipients (n = 6 mice per cell type and genotype). Data show peripheral blood counts in recipients of CD41^{hi} or CD41^{lo} HSCs (top row) and donor chimerism determined as a percentage of GFP⁺ cells in PB (bottom row). Spleen weights of CD41^{hi} and CD41^{lo} HSC transplant-recipient mice at 24 weeks after transplantation are shown (top right graph). Group size: n = 6 mice per cell type and genotype. (D) Analysis of donor chimerism (percentage of GFP⁺ cells) in progenitor and stem cells in BM and spleen in CD41^{hi} and CD41^{lo} HSC transplant recipients at 24 weeks after transplantation (n = 6 mice per cell type and genotype). (E) Analysis of recipients of CD41^{lo} HSC transplants. Stacked bar graph shows percentages of CD41^{lo} and CD41^{hi} HSCs in the GFP⁺ subset of LT-HSCs. One- or 2-way analyses of variance followed by Tukey's multiple-comparisons test were used for multiple-group comparisons. All data are means \pm standard error of the mean. *P < .05; **P < .01; ***P < .001; ****P < .0001.

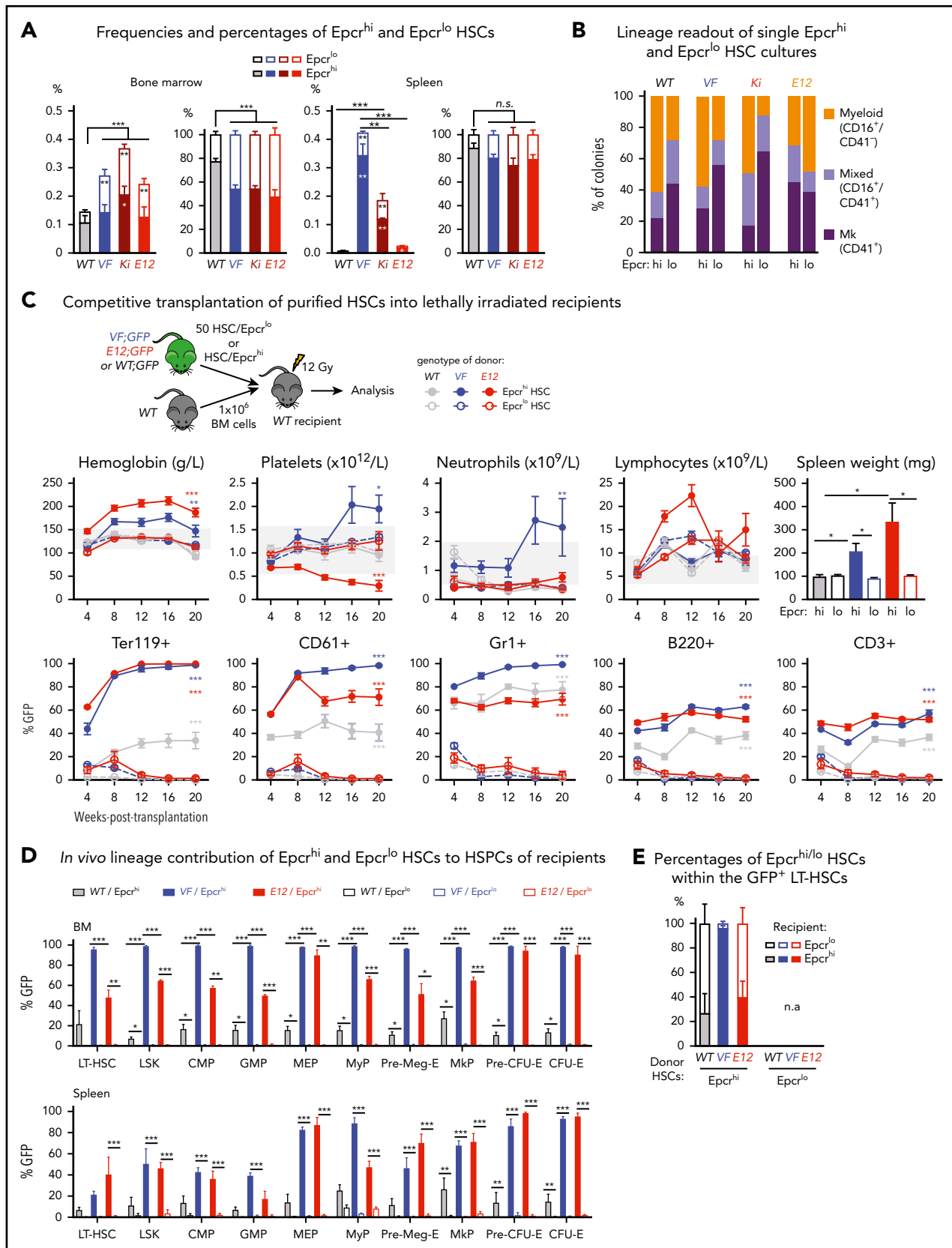


Figure 2. Expression analyses and functional characterization of Epcr^{hi} and Epcr^{lo} HSCs revealed an inverse correlation with CD41 expressing HSC subsets. (A) Frequencies (left) and percentages (right) of Epcr^{hi} and Epcr^{lo} HSCs within the phenotypic HSC compartment in BM and spleen of the indicated genotypes (n = 7-12 mice). (B) Analysis of colonies grown from FACS-sorted single Epcr^{hi} and Epcr^{lo} HSCs in liquid culture showing the percentages of colonies containing Mk (CD41⁺), myeloid (CD16⁺), or mixed (Mk and myeloid, CD41⁺/CD16⁺) cells after 10 days of culture (n = 128 cells per cell type/genotype and n = 3 mice). (C) Competitive BM transplantation. Hematopoietic

HSCs showed normal blood counts without splenomegaly (Figure 1C). Recipients of CD41^{lo} HSCs showed higher GFP chimerism than recipients of CD41^{hi} HSCs in all lineages of PB (Figure 1C) and also higher contribution to HSC and progenitor compartments in BM and spleen (Figure 1D). In BM of recipients transplanted with CD41^{lo} HSCs, we found that most GFP⁺ (V617F-expressing) HSCs retained the original CD41^{lo} phenotype, but ~20% converted to CD41^{hi} (Figure 1E), demonstrating that CD41^{lo} HSCs can convert to CD41^{hi} HSCs. Because of the lack of long-term engraftment, this analysis was not feasible in recipients of CD41^{hi} HSCs. Thus, Mk-biased (CD41^{hi}) HSCs preferentially contributed to megakaryopoiesis in vitro, and they were impaired in their lineage output and long-term repopulation capacity in vivo.

Expression of CD41 on subsets of HSCs inversely correlated with expression of EPCR

Expression of *Epcr* (*Procr1*) was described as a marker of quiescent HSCs.^{9,10} We found that the expression of *Epcr* mRNA and protein in HSCs inversely correlated with CD41 (supplemental Figure 2A). These data suggested that *Epcr*^{hi} HSCs may be phenotypically and functionally comparable with CD41^{lo} HSCs. Indeed, we found a decrease in the percentages of *Epcr*^{hi} HSCs in BM and spleen of *JAK2* mutant mice (Figure 2A; supplemental Figure 2B). We also found an ~20-fold increase of circulating LSKs and HSCs in *VF* mice that were mostly *Epcr*^{lo} (supplemental Figure 2C-D), consistent with earlier findings in mice.¹⁰

Liquid cultures of single-cell-sorted *Epcr*^{lo} HSCs from *VF*, *Ki*, and *WT* (but not *E12*) mice produced higher percentages of Mk colonies than sorted *Epcr*^{hi} HSCs produced (Figure 2B). Overall, the pattern of lineage output of *Epcr*^{lo} and *Epcr*^{hi} HSCs was converse to that of CD41^{lo} and CD41^{hi} HSCs (Figure 1B; supplemental Figure 2E). We also determined the reconstitution potential of *Epcr*^{lo} and *Epcr*^{hi} HSC subsets in competitive transplantations in vivo. We transplanted FACS-sorted HSCs along with 1×10^6 total BM competitor cells into lethally irradiated recipient mice (Figure 2C). Recipients of *Epcr*^{hi} HSCs from *JAK2* mutant donor mice showed high GFP-chimerism and also developed MPN phenotype (Figure 2C). In contrast, *Epcr*^{lo} HSC could not sustain long-term hematopoiesis and were out-competed by the *WT* competitor cells. Only recipients of *Epcr*^{hi} HSCs maintained GFP-chimerism at terminal workup 20 weeks after transplantation (Figure 2D). We determined the ratio of *Epcr*^{hi} to *Epcr*^{lo} in the GFP⁺ fraction of HSCs from BM (Figure 2E). Although in recipients of *WT* and *E12* HSCs more than half of the originally *Epcr*^{hi} HSCs converted to *Epcr*^{lo} phenotype, in *VF* recipients almost all HSCs retained the original *Epcr*^{hi} phenotype, because of the lack of long-term engraftment, this analysis was not feasible in recipients of *Epcr*^{lo} HSCs. Thus, the CD41^{lo} and *Epcr*^{hi} HSCs were functionally similar in having competitive advantage and higher long-term repopulating activity.

Transcriptional profiling of CD41^{hi} and CD41^{lo} HSCs

To gain insights into the cellular and molecular identity and the signaling pathways active in Mk-biased HSCs, we performed RNA sequencing of total HSCs, CD41^{hi} and CD41^{lo} HSC subsets, bipotent megakaryocyte erythroid progenitors (MEPs), and committed megakaryocyte progenitors (MkPs; Figure 3A). Principal component analysis (PCA) revealed that CD41^{hi} and CD41^{lo} HSCs in *WT* mice clustered closer with unfractionated total HSCs than with MEPs or MkPs (Figure 3B). In *VF* mice, the unfractionated HSCs and the CD41^{hi} and CD41^{lo} subsets of HSCs each clustered farther apart, but were clearly distinct from MEPs and MkPs. CD41^{hi} and CD41^{lo} HSCs from *WT* and *VF* mice fell into 4 separate clusters (Figure 3C). The number of differentially expressed genes between CD41^{hi} vs CD41^{lo} HSCs are shown in Figure 3D. Gene Set Enrichment Analysis (GSEA) on differentially regulated genes between CD41^{hi} and CD41^{lo} HSCs revealed that *E2F* targets, *G₂/M* checkpoint, *Myc*, *mTORC1*, and oxidative phosphorylation pathways were among the top upregulated gene pathways in CD41^{hi} HSCs, whereas CD41^{lo} HSCs had higher gene expression of inflammatory signaling pathways, such as *IFN α* , *IFN γ* , *IL-6* *JAK/STAT*, and *TNF α /NF κ B* (Figure 2E). Most of these differentially expressed gene pathways were found in both *WT* and *VF* genotypes.

Comparison of gene expression in CD41^{hi} vs CD41^{lo} HSCs, using a selected set of genes thought to play a role in HSC maintenance and Mk lineage regulation is shown in Figure 3F.^{2,4} As expected, expression levels of *Itga2b* (CD41) was higher in CD41^{hi} HSCs and conversely, expression of *Procr* (*Epcr*) was higher in CD41^{lo} HSCs (Figure 3F, red). Consistent with previous reports,^{2,4} CD41^{hi} HSCs, irrespective of *VF* or *WT* genotype, also displayed elevated expression of megakaryocyte/platelet lineage regulators *Clu*, *VWF*, *Gp1bb*, *Gp5*, and *Aurka* than CD41^{lo} HSCs. CD41^{hi} HSCs also expressed *Pf4* (*Cxcl4*), a known Mk lineage marker that was thought be exclusively expressed by later MK lineages, but recently was also detected in HSCs.²³ Expression levels of Mk/platelet lineage regulator genes normalized to *WT* CD41^{lo} HSCs (set as 1) are shown in Figure 3G. Together with the in vitro and in vivo functional testing, the molecular analysis suggests that CD41^{hi}/*Epcr*^{lo} HSCs are not lineage-restricted progenitors, such as MEPs or MkPs, but rather represent a subset of HSCs.

CD41^{hi} /*Epcr*^{lo} HSC subset display increased cell cycle activity and augmented oxidative phosphorylation

We used single-cell tracking of sorted HSCs and found that HSCs from *VF* mice entered the first and second cell divisions earlier than *WT* controls or *E12* mice (Figure 4A). Because RNA sequencing showed prominent differences between CD41^{hi}/*Epcr*^{lo} and CD41^{lo}/*Epcr*^{hi} HSC subsets in expression of cell cycle regulators, we compared their cell cycle status by flow cytometry. In *WT* mice, a lower percentage of CD41^{hi}/*Epcr*^{lo} HSCs were

Figure 2 (continued) lineage contributions of GFP⁺ *Epcr*^{hi} and *Epcr*^{lo} HSCs in the PB of recipients. Peripheral blood counts (top row) and donor derived (percentage of GFP⁺) cells (bottom row; n = 6 mice per genotype). Spleen weights of *Epcr*^{hi} and *Epcr*^{lo} HSC transplant recipients at 24 weeks after transplantation are shown (top right; n = 6-8 mice per cell type and genotype). (D) In vivo lineage contribution of *Epcr*^{hi} and *Epcr*^{lo} HSCs to HSPCs in transplant-recipient mouse BM and spleen at 24 weeks after transplantation (n = 4-6 mice cell type and genotype). (E) Percentages of *Epcr*^{hi} and *Epcr*^{lo} HSCs within the GFP⁺ subset of BM cells in transplant recipients at 24 weeks after transplantation. Note that only recipients of *Epcr*^{hi} HSC transplants were analyzed, because, at 24 weeks, recipients of *Epcr*^{lo} HSCs did not show GFP⁺ engraftment. All data are means \pm standard error of the mean. **P* < .05; ***P* < .01; ****P* < .001.

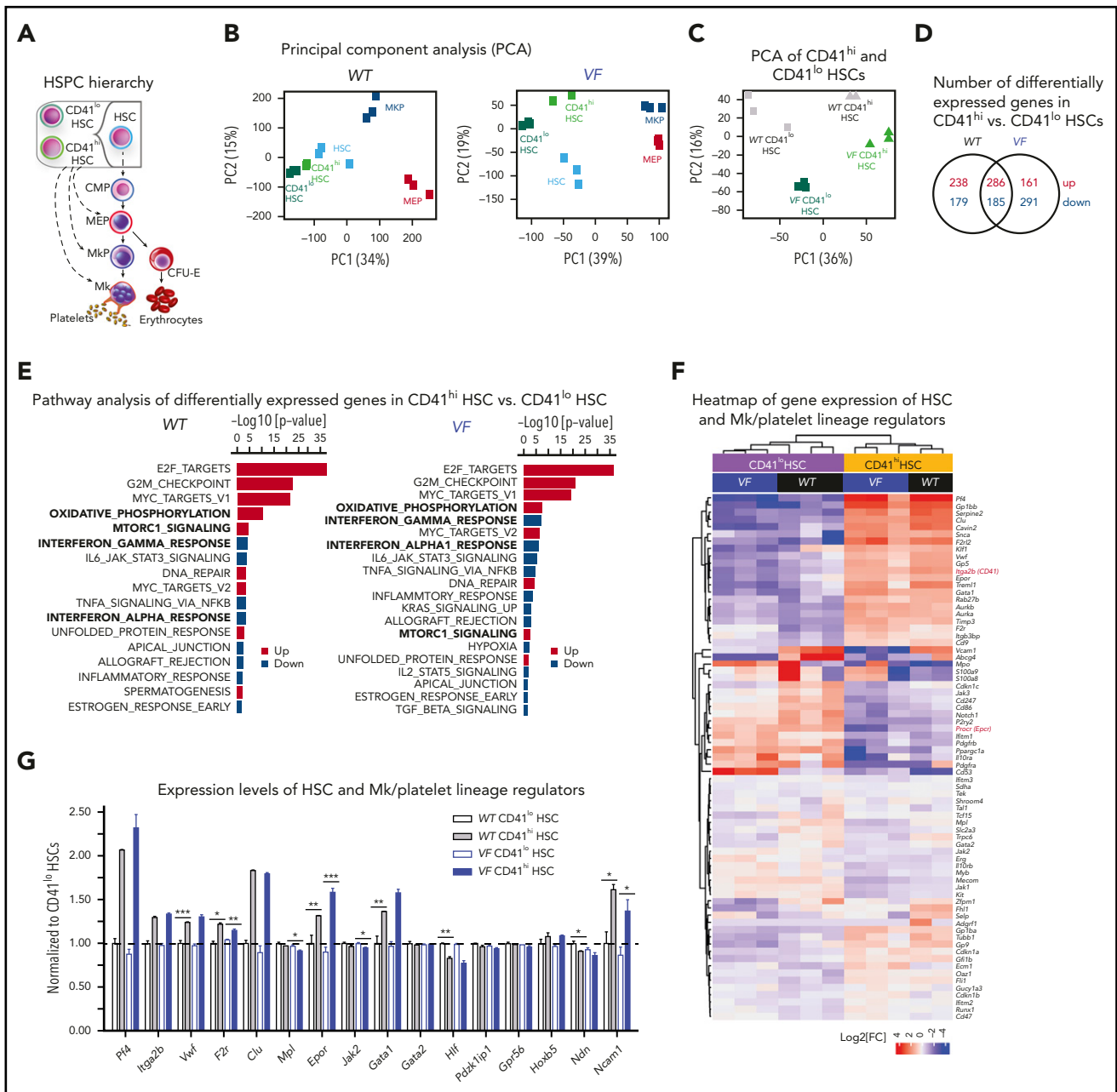


Figure 3. RNA sequencing profiling of CD41^{hi} and CD41^{lo} HSCs. (A) Stem and progenitor (HSPC) hierarchy. (B) PCA of the indicated HSPC subsets from WT and VF mice revealed transcriptional hierarchy within the HSPCs. (C) PCA of CD41^{hi} and CD41^{lo} HSC subsets from WT and VF mice. (D) The number of shared and differentially expressed genes in CD41^{hi} and CD41^{lo} HSC subsets between the WT and VF groups (false discovery rate [FDR] < .05 and fold change > 1.5). (E) GSEA of differentially expressed molecular pathways from the MSigDB hallmark gene sets in CD41^{hi} and CD41^{lo} HSC subsets from WT and VF mice (FDR < .05). (F) Heat map of Mk/platelet lineage regulator expression in CD41^{hi} and CD41^{lo} HSC subsets from WT and VF mice (FDR < .05 and fold change > 1.5). (G) Normalized expression levels of selected genes involved in HSC and Mk/platelet lineage regulation. The results obtained in CD41^{lo} HSCs were set to 1 and compared with the corresponding values obtained in CD41^{hi} HSCs. Data are means \pm standard error of the mean. *P < .05; **P < .01; ***P < .001.

quiescent in the G₀ phase, and a higher percentage of cells were in the G₁/S phases compared with CD41^{lo}/Epcr^{hi} HSCs. These differences were even more pronounced in mutant JAK2-expressing mice (Figures 4B-C). Consistently, CD41^{hi} HSC subset showed higher expression of cell cycle activators *Cdk1*, *Cdk2*, *Cdk4*, *Cdk6*, and *cyclin E1*, and lower expression of cell cycle inhibitors *Cdkn1c* (p57) compared with the CD41^{lo} HSC subset (supplemental Figure 3), suggesting that CD41^{hi} HSCs represent an activated subset of phenotypic HSCs.

In addition, we noted that CD41^{hi}/Epcr^{lo} HSCs were larger than CD41^{lo}/Epcr^{hi} HSCs, as indicated by higher forward scatter (size) values (Figure 4D). Interestingly, the CD41 and Epcr antibody labeling appeared to be polarized and forming caps in CD41^{lo}/Epcr^{hi} HSCs (Figure 4E). Furthermore, as a consequence of augmented oxidative phosphorylation we found that CD41^{hi}/Epcr^{lo} HSCs harbored higher levels of reactive oxygen species (ROS) compared with CD41^{lo}/Epcr^{hi} HSCs (Figure 4F). Using the dye Mitotracker Green, we detected increased mitochondria mass in Epcr^{lo} HSCs compared with the Epcr^{hi} subset (Figure 4G),

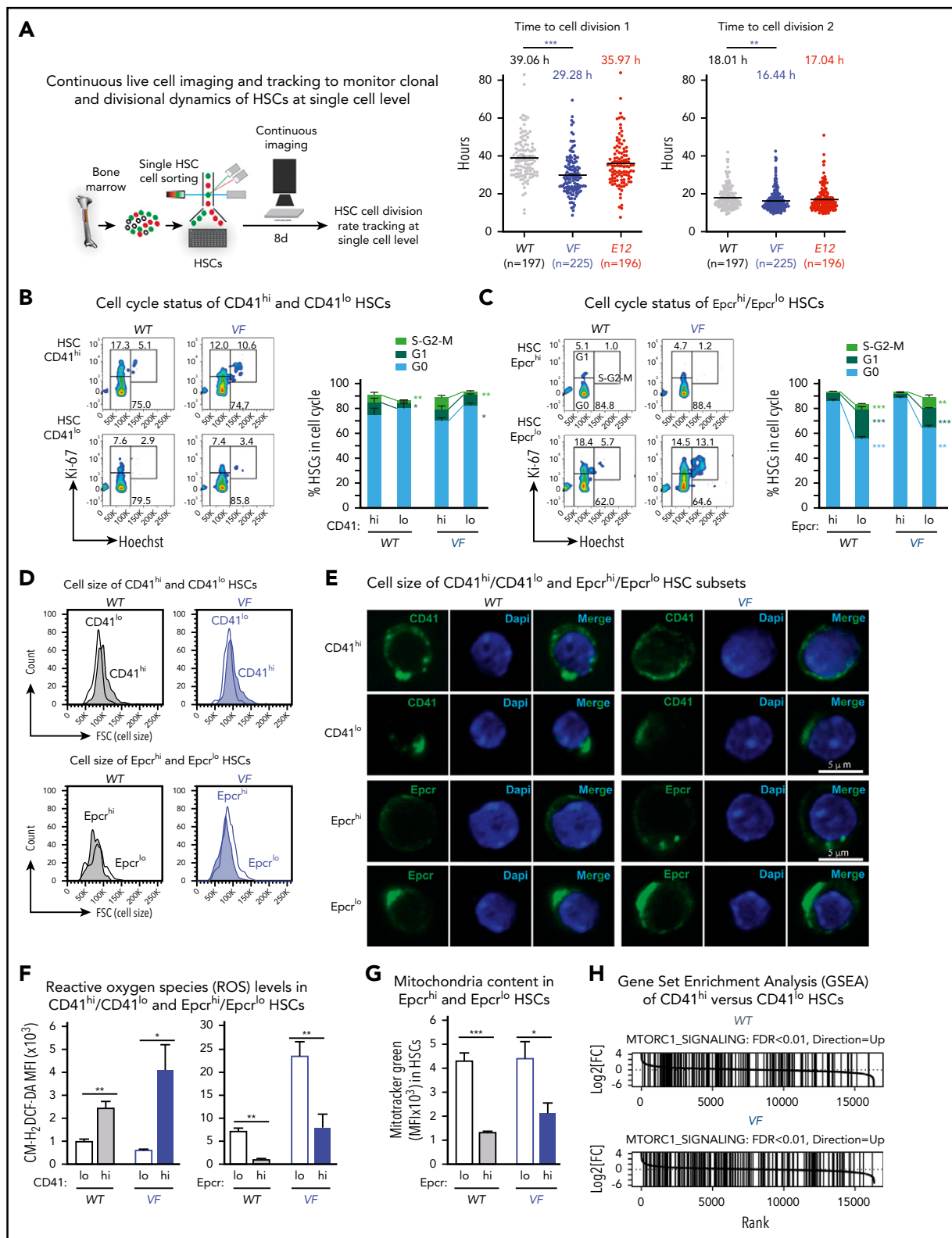


Figure 4. CD41^{hi}/Epcr^{lo} HSCs display enhanced cell cycle activity, increased mitochondrial content, and augmented mTOR signaling signature. (A) Experimental setup for measuring time to first cell division by single-cell tracking of sorted HSCs. (B,C) Dot plots show the time to the first and second cell divisions. Cell cycle status of CD41^{hi} and CD41^{lo} HSCs (B) and Epcr^{hi} and Epcr^{lo} HSCs (C). Increased percentage of Epcr^{lo} and CD41^{hi} HSCs reside in G₁ and S phases (WT, n = 4 mice; VF, n = 7 mice). (D) Cell size of Epcr^{hi} and Epcr^{lo} HSCs (top) and CD41^{hi} and CD41^{lo} HSCs (bottom) assessed by the forward scatter parameter in flow cytometry (n = 6 mice per genotype). (E) Confocal microscopy of CD41^{lo} and CD41^{hi} HSCs and Epcr^{hi} and Epcr^{lo} HSCs revealed increased cell size of the Epcr^{hi} and CD41^{lo} HSC subsets. (F) ROS levels in Epcr^{hi}/Epcr^{lo} and CD41^{hi} and CD41^{lo} HSC subsets showing CM-H₂DCF-DA mean fluorescence intensity (MFI; n = 6 mice per genotype). (G) Mitochondria content in Epcr^{hi} and Epcr^{lo} HSCs detected with Mitotracker Green MFI (n = 6 mice per genotype). (H) GSEA of CD41^{hi} and CD41^{lo} HSCs showing increased expression of genes involved in mTOR signaling in CD41^{hi} vs CD41^{lo} HSCs (false discovery rate < .01). All data are means ± standard error of the mean. *P < .05; **P < .01; ***P < .001.

consistent with CD41^{hi}/Epcr^{lo} HSCs being the metabolically more active HSC subset. Increased cell size, enhanced activation of HSCs from quiescence, and active metabolism are some of the hallmark signatures of active mTOR signaling.²⁴ Indeed, GSEA analysis highlighted Raptor (mTORC1), an essential component of mTOR signaling, as one of the upregulated pathways in CD41^{hi} HSC subset (Figure 4H). Collectively, these data confirm the differences derived from RNA sequencing analysis.

Increased percentages of CD41^{hi} of hematopoietic stem and progenitor cells in the BM of patients with MPN

To determine whether the markers for Mk-biased HSCs can also be used in human MPN, we assessed the percentages of CD41^{hi} hematopoietic stem and progenitor cells (HSPCs) in the BM of patients with MPN and healthy controls (Figure 5A; supplemental Figure 4). Similar to our findings in mice, the human CD41^{hi} HSPCs also displayed increased size (supplemental Figure 5A). The percentage of CD41^{hi} HSCs in BM from healthy controls (n = 7) was very low (1.4% ± 0.45% standard error of the mean [SEM]; Figure 5A, left). Of note, HSCs derived from cord blood (n = 8) showed a substantially higher percentage of CD41^{hi} HSCs (11.2% ± 9.5% SEM) than did BM from healthy adult controls (supplemental Figure 5B), illustrating differences between HSPCs from cord blood and BM. The percentages of CD41^{hi} HSCs in BM of patients with MPN (n = 29) was significantly increased 20.4% ± 4.0% SEM (P = .001; Figure 5A, left). The percentages of CD41^{hi} cells were also elevated in common myeloid progenitors (CMP), granulocyte macrophage progenitors (GMP), and MEP, and this increase was again greater in patients with MPN (35% to 40%) than in healthy controls (~12%; Figure 5A).

Within the MPN subgroups, PV patients had the highest percentage of CD41^{hi} HSPCs, followed by PMF and essential thrombocythemia. We found a correlation between the percentages of CD41^{hi} HSPCs in the BM of patients with MPN and the corresponding JAK2-V617F allele burden in PB granulocytes (Figure 5B). These results suggest that expression of JAK2-V617F may be primarily responsible for the expansion of CD41^{hi} HSCs. Increased percentages of CD41^{hi} HSPCs in the BM of patients with MPN did not correlate with increasing age (supplemental Figure 5C-D), contrary to a previous report that found an age-dependent increase in CD41^{hi} HSCs in older WT mice.³ We performed single-cell liquid cultures of FACS-sorted CD41^{hi} and CD41^{lo} HSCs and CMPs from 4 patients with MPN. Approximately 50% of HSC- and CMP-derived colonies were JAK2-V617F⁺ by allele-specific polymerase chain reaction (PCR; Figure 5C). The JAK2-V617F⁺ CD41^{hi} HSCs gave rise to a significantly higher percentage of pure Mk colonies (all CD41⁺ cells) compared with CD41^{lo} HSCs, but this difference was not observed in WT CD41^{hi} vs CD41^{lo} HSCs (Figure 5C). Colonies derived from CD41^{hi} CMPs were predominantly of pure Mk phenotype irrespective of the genotype. (Figure 5C, right). Overall, the Mk output of JAK2-mutant HSCs in vitro was similar as observed in the experiments using sorted mouse VF and Ki HSCs (Figure 1B). Collectively, these data indicate that changes induced by expression of mutant JAK2 cause expansion of Mk-biased HSCs in MPN mouse models and patients with MPN, and their frequency was significantly associated with the JAK2-V617F mutant allele burden.

We also examined the expression of EPCR on human BM cells. However, HSCs from healthy controls were almost exclusively EPCR^{lo} (supplemental Figure 6). Thus, in contrast to mice, the expression of EPCR in humans did not inversely correlate with the expression of CD41 and we therefore used CD41 as a marker to further characterize human Mk-biased HSCs.

Interferon signaling induces expansion of CD41^{hi} HSCs in mice

Type 1 interferons (IFN- α , IFN- β) and type 2 interferons (IFN- γ) were shown to promote cell cycle entry and induce differentiation of quiescent HSCs.^{17,25} RNA sequencing showed increased expression of IFN pathway genes in CD41^{lo} HSCs (Figure 3E; supplemental Figure 7A-B), suggesting that CD41^{lo} HSC subsets may be more responsive to IFN stimuli. To examine the effects of IFN on CD41 subsets of HSCs in vivo, we treated VF and WT mice with plpC, an IFN-inducing agent.^{17,25,26} Injection of a single dose of plpC significantly increased the percentage of CD41^{hi} HSCs within 24 hours in both VF mice and WT mice (Figure 6A; supplemental Figure 8).^{19,27} This response to plpC was completely abolished in VF and WT mice genetically deficient in the IFN receptor (*Ifnr1*; Figure 6A).²² Interestingly, loss of *Ifnr1* also lowered the baseline percentages of CD41^{hi} cells in VF;*Ifnr1*^{-/-} mice to the levels found in WT mice, indicating that the increased baseline in VF mice also requires IFN signaling. Indeed, IFN- β levels were elevated in BM lavage of VF and Ki mice compared with WT (supplemental Figure 7C), suggesting that the observed JAK2-V617F-induced IFN response is indirect and mediated by increased levels of type 1 IFN family members.

Similarly, plpC treatment also decreased the percentages of Epcr^{hi} HSC subsets in both VF and WT mice (Figure 6B). Loss of *Ifnr1* reduced the effect of plpC, although a trend toward lower percentages of Epcr^{hi} HSC remained, suggesting that plpC can induce *Ifnr1* independent signaling events. Thus, short-term IFN signaling in JAK2 mutant mice increased the fraction of CD41^{hi}/Epcr^{lo} Mk-biased HSCs. A single dose of Tpo increased the percentage of CD41^{hi} HSCs in WT and VF mice (supplemental Figure 8C), indicating that the phenotypic shift to CD41^{hi} is not specific to the mutant JAK2. Contrary to expectations, Tpo in the same experiment did not reduce the percentages of Epcr^{hi} HSCs in WT or VF mice, demonstrating that CD41 and Epcr subpopulations of HSCs do not always behave reciprocally. This result was not related to alterations in the expression of IFN-dependent cell surface markers such as Sca-1,²⁸ as demonstrated by expression of another HSC marker, Esam-1,^{29,30} on nearly all CD41^{lo} and CD41^{hi} HSC subsets (supplemental Figure 9).

Long-term IFN treatment increases the fraction of CD41^{hi} HSCs and leads to exhaustion of HSCs

We expected that augmenting the CD41^{hi} HSCs fraction by IFN- α will eventually lead to a decrease in the JAK2 mutant clone size. We tested this hypothesis in mice by competitive BM transplantations of BM cells from VF mice that coexpress the GFP reporter mixed with WT BM cells in a 1:1 ratio (Figure 6C). Recipient mice were allowed to engraft and reconstitute for 6 weeks and were then treated with pegylated IFN- α (pegIFN- α), which has a longer half-life in the circulation than native IFN- α ³¹ or vehicle only (Figure 6C). Consistent with its known therapeutic effects in patients with MPN, pegIFN- α treatment significantly reduced hemoglobin levels, platelet counts, and spleen size.

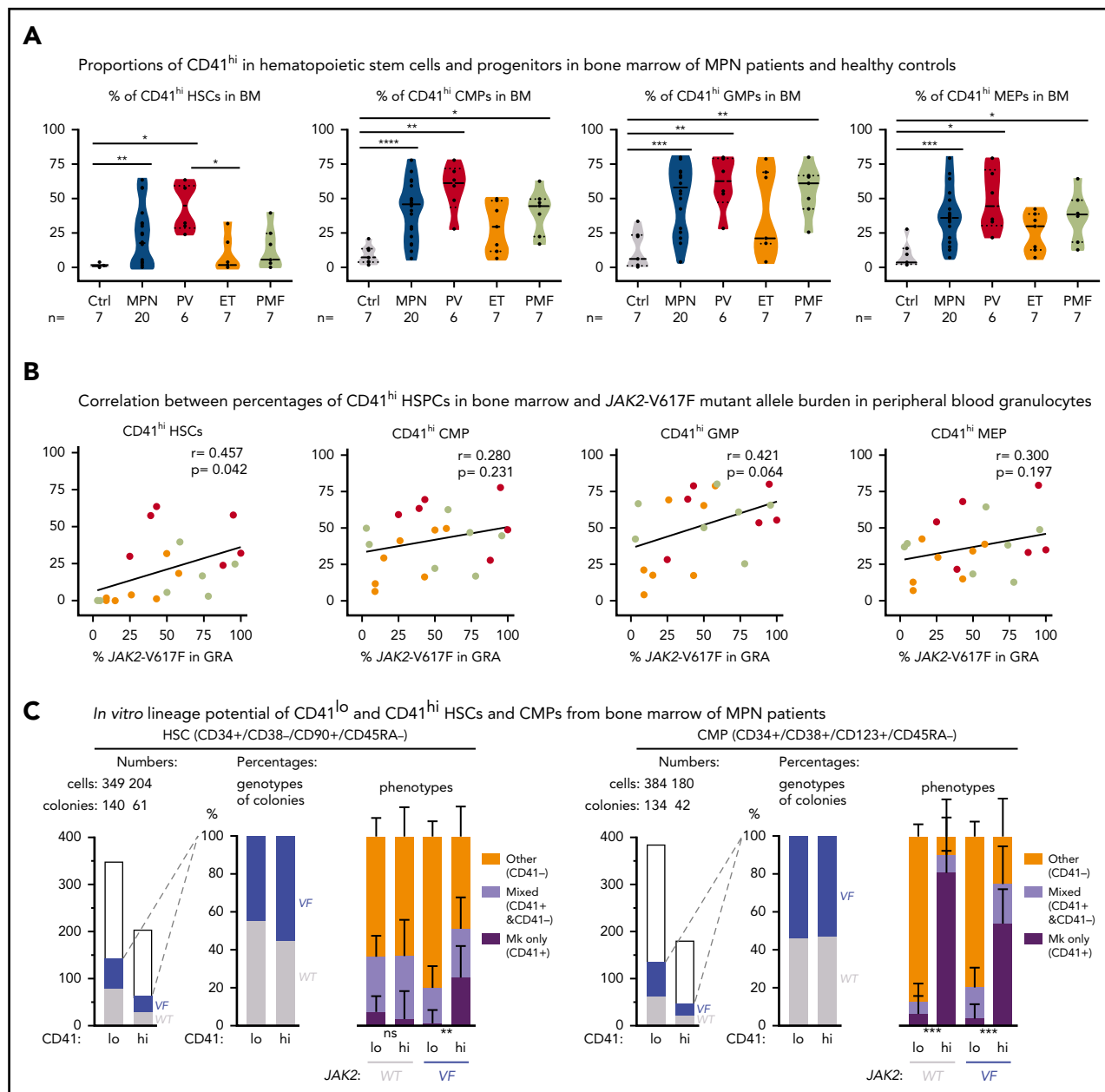


Figure 5. Increased abundance of CD41⁺ HSPCs in the BM of patients with MPN. (A) Violin plots showing percentages of CD41^{hi} HSC, CMP, GMP, and MEP progenitor cells in the BM of controls (n = 7) and patients with MPN (n = 29). Unpaired t test with Welch's correction. (B) Correlation (r, Pearson correlation) and significance (2-tailed Student t test) between mutant allele burden measured in PB granulocytes and percentages of CD41⁺ HSPCs in the BM were calculated and are shown for JAK2-V617F⁺ patients only. (r, Pearson correlation; P, 2-tailed Student t test). No correlation was observed in patients with the CALR mutation. (C) *In vitro* lineage potential of CD41^{lo} and CD41^{hi} HSCs and CMPs. FACS-sorted single cells were grown in 384-well plates, and, after 14 days of culture, colonies were first phenotyped inside the wells by CD41 antibody staining and live microscopy and then genotyped by allele-specific polymerase chain reaction (PCR) for JAK2-V617F. Combined data from 4 JAK2-V617F⁺ patients with MPN (2 PV and 2 PMF) are shown, along with the number of CD41^{lo} and CD41^{hi} single cells plated and the number of colonies with WT (gray) and JAK2-V617F (VF; blue) genotypes (left) and the percentages of VF vs WT colonies and the percentages of Mk colonies (all cells CD41⁺), mixed colonies (CD41⁺ and CD41⁻ cells present in the same colony), and colonies with other phenotypes (all cells CD41⁻ in the same colony) (right). Differences in lineage proportions between CD41^{lo} and CD41^{hi} populations were tested by Fisher's exact test with the Hochberg correction for multiple testing. All data are means ± standard error of the mean; ns, not significant; *P < .05; **P < .01; ***P < .001; ****P < .0001.

At terminal workup after 22 weeks, mice treated with pegIFN- α also showed decreased JAK2-V617F mutant allele burden in HSCs, as indicated by reduced frequencies and percentages of GFP⁺ HSCs in BM and spleen (Figure 6D). The total frequencies of HSCs increased in the pegIFN- α -treated mice, but this was because of an increase in GFP⁻ (WT) HSCs. In the GFP⁺ (JAK2-mutant) fraction of HSCs, the pegIFN- α -treated mice showed an increase in the percentages of CD41^{hi} HSCs. Interestingly, in the

BM of vehicle-treated mice, the GFP⁻ HSCs (but not in the spleen) were almost 100% CD41^{hi}, suggesting that the presence of the JAK2-V617F (GFP⁺) cells had an influence on the CD41 phenotype of the WT HSCs. The JAK2-WT HSPCs responded to pegIFN- α by increasing in total frequencies and the percentages of the CD41^{lo} subsets, suggesting that they recover from the damaging presence of the JAK2-V617F expressing cells. This notion is supported by the histological findings of improved BM

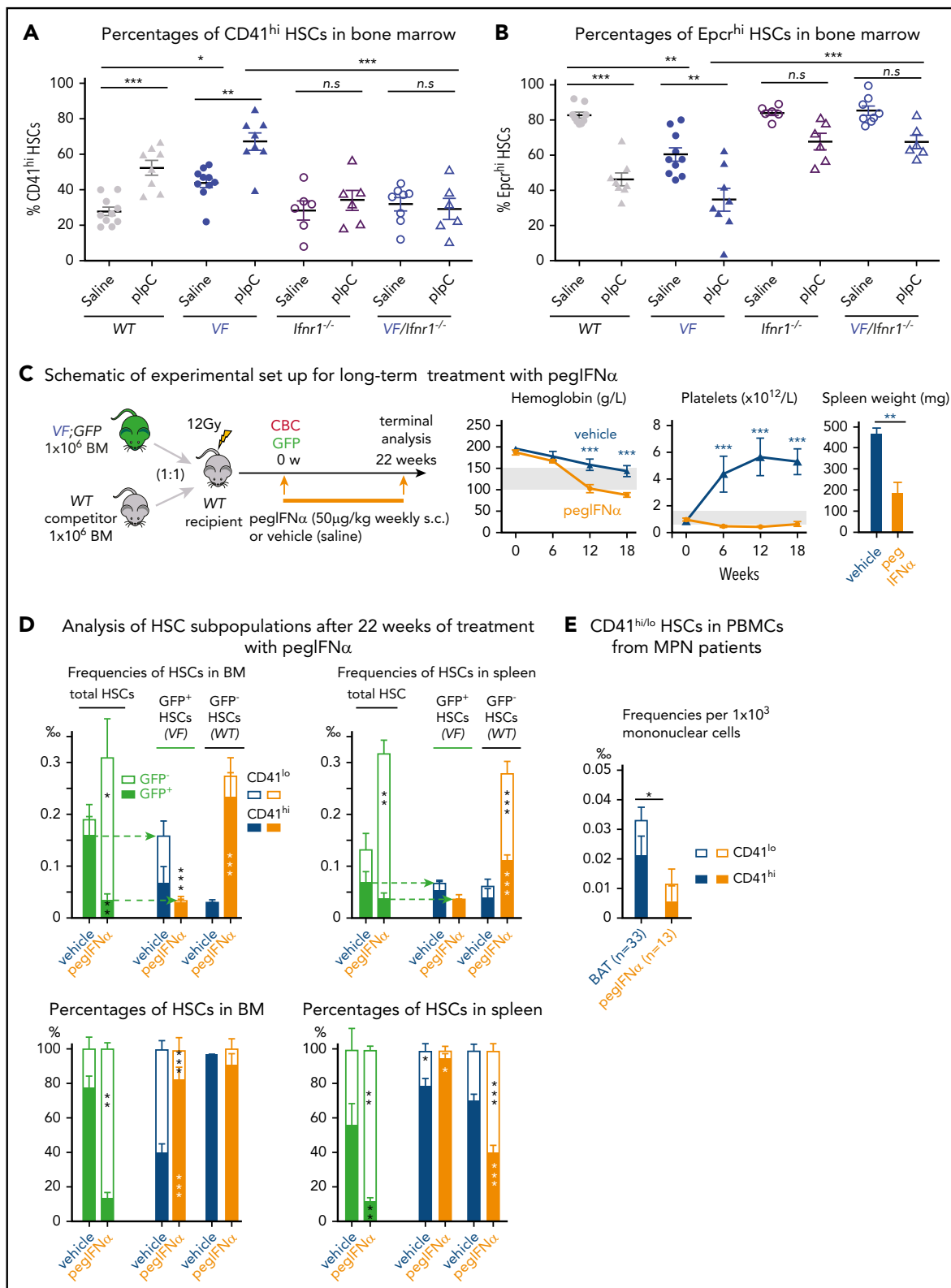


Figure 6. Prolonged IFN treatment induces depletion of quiescent HSCs via continuous induction of CD41^{hi} HSC subset. (A-B) Percentages of CD41^{hi} and Epcr^{hi} HSCs in the BM after 24 hours of saline or plpC treatment in mice with the indicated genotypes (2-way analysis of variance [ANOVA]). (C) Competitive BM transplantation and pegIFN- α treatment regimen, with hemoglobin levels and platelet counts in the PB of pegIFN- α - or vehicle-treated recipient mice and spleen weight in the recipient mice at 22 weeks after the treatment (n = 5 mice per group). (D) Analysis of HSC subpopulations after 22 weeks of treatment in BM and spleen of pegIFN- α - or vehicle-treated, transplant-recipient mice. Gating on GFP⁺ cells enabled determination of the CD41^{hi/lo} ratios selectively in JAK2-mutant (VF) vs GFP⁻ HSCs. Shown are the frequencies (top) and percentages (bottom) of HSC subsets (n = 5 mice per genotype). Statistical significance between pegIFN- α - and vehicle-treated mice was derived by 2-way ANOVA. (E) Frequencies and percentages of CD41^{hi} and CD41^{lo} HSCs in PBMCs of pegIFN- α -treated (n = 13) and control patients with MPN receiving best available therapy (BAT; n = 33). Unpaired Student t test with Welch's correction. All data are means \pm standard error of the mean. *P < .05; **P < .01; ***P < .001.

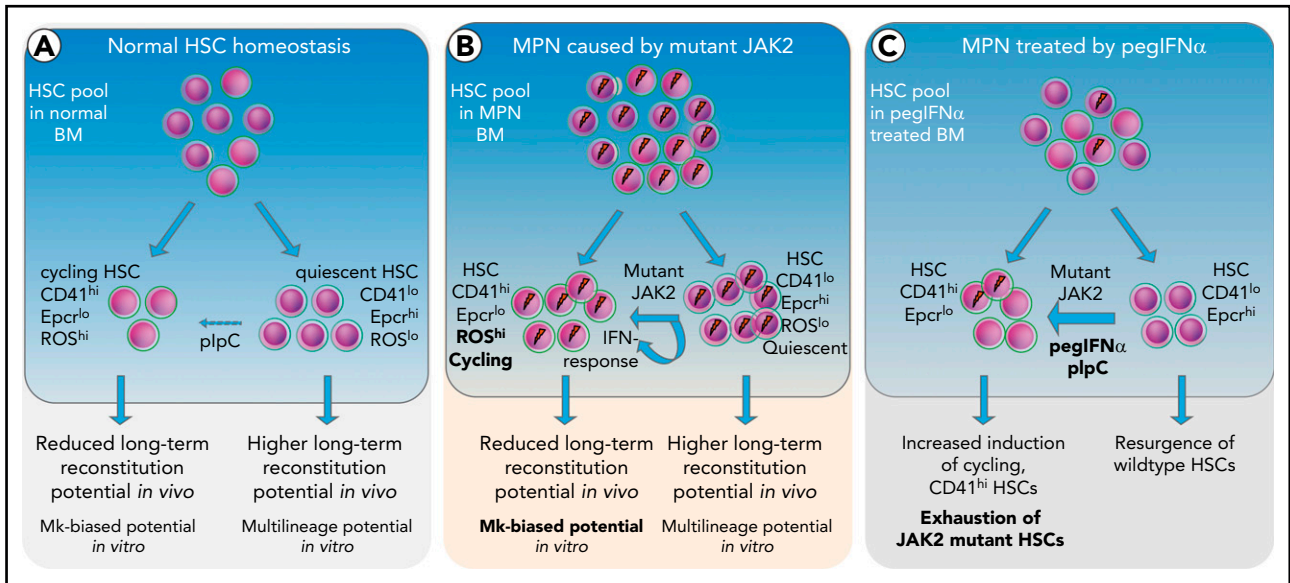


Figure 7. Model depicting the effects of mutant *JAK2* and *IFN-α* on the proportion of megakaryocyte-biased (*CD41^{hi}*) HSCs. (A) HSC homeostasis in BM of WT mice. The proportion of *CD41^{hi}* HSCs is low (~30%). (B) HSC pool in MPN mice expressing mutant *JAK2*. The proportion of *CD41^{hi}* HSCs is increased (≤50%) because of the expression of mutant *JAK2*. *CD41^{hi}* HSCs in mice are characterized by lower *Epcr* expression, active cell cycle state, increased cell size, increased ROS levels, reduced long-term reconstitution potential *in vivo*, and Mk-biased potential *in vitro*. The effect of the mutant *JAK2* on *CD41* subset is mediated by the *VF*-induced *IFN* response and requires the presence of *Ifnr1*. (C) Summary of alterations in the HSC compartment of mice or patients with MPN treated with pegIFN α .

morphology in the pegIFN- α -treated group (supplemental Figure 10). These results suggest that IFN- α preferentially reduces *JAK2*-V617F (*GFP⁺*) HSCs by increasing the proportion of *CD41^{hi}* subset of HSCs (Figure 6D). The converse changes were observed when *Epcr* expression was analyzed instead of *CD41* (supplemental Figure 11). Similar effects of pegIFN- α as in LT-HSCs were also observed in ST-HSCs and MPPs (supplemental Figure 11D-E).

We also compared HSC numbers and *CD41^{hi}* vs *CD41^{lo}* phenotypes in PB of 13 patients with MPN treated by pegIFN- α with 33 patients with MPN receiving best available therapy. We observed lower frequencies of phenotypic HSCs in the pegIFN- α -treated group (Figure 6E).

Based on the data, we propose a model (Figure 7), in which short-term exposure of HSCs to IFN induces cell cycle entry and conversion from *CD41^{lo}* to *CD41^{hi}* Mk-biased HSCs. Prolonged chronic exposure to pegIFN- α results in depletion of *JAK2*-mutant HSCs via continuous conversion of *CD41^{lo}* to the *CD41^{hi}* HSC subset.

Discussion

Our study provides insights into the functional properties of Mk-biased HSCs in the context of *JAK2*-mutated MPN. We found that expression of mutant *JAK2* increased the frequency and percentage of the *CD41^{hi}* subset of HSCs in mouse models of MPN. *CD41^{hi}* HSCs displayed reduced competitiveness for long-term reconstitution in competitive transplantation assays. *CD41* was also a valid marker for Mk-biased HSCs in patients with *JAK2*-mutated MPN. In addition, we found that expression of *Epcr*, a marker for quiescent HSCs was inversely correlated with the *CD41* expression on HSCs in mice, but not in patients with

MPN. The basis for the differences in *EPCR* expression patterns between mice and humans is currently unknown.

CD41^{hi} HSCs are actively proliferating, lineage-primed cells and could represent a fraction of the previously reported *VWF⁺* HSCs,² or G (Alert) state HSCs.²⁴ *CD41^{hi}* HSCs displayed higher ROS levels and higher mitochondrial content, in agreement with a previous report that *WT* HSCs with high mitochondrial activity exhibited megakaryocytic lineage differentiation *in vitro*³² and is consistent with our previous report on altered metabolic activity in mutant *JAK2*-expressing HSCs.^{33,34} There is no consensus in the field as to whether these cells should be called HSCs.^{1,4} A recent study challenged the existence and relationship of Mk-biased HSCs with phenotypic HSCs.³⁵ Using *in vitro* single-cell assays the results in study indicated that Mk progenitors are not directly derived from HSCs, but rather share a similar surface marker phenotype and may represent merely an impurity of myeloid progenitors among HSCs. Our RNA sequencing data of the *CD41^{hi}* subset showed features typical of HSCs and in our *in vivo* functional assays, the *CD41^{hi}* subset gave rise to multilineage contribution, but did not sustain long-term hematopoiesis.

IFN- α treatment is the only therapy known to induce molecular remission in a subset of patients with MPN,¹⁶ but the mechanism of IFN action in MPN remains unclear. In mice, IFN- α treatment was shown to reduce the number of HSCs, suggesting that IFN- α acts by exhausting the *JAK2* mutant HSCs.^{19,27,36,37} Our study provides further insight into the possible mechanism by showing that long-term treatment with pegIFN- α preferentially increased the frequency and percentage of *CD41^{hi}* HSCs in *JAK2*-V617F-expressing HSCs. This leads to a model of how IFN- α , in combination with *JAK2*-V617F, induces HSC cycling,¹⁵ could selectively reduce the *JAK2* mutant clone (Figure 7). Our study does not exclude other cellular targets by which IFN- α could

mediate disease-modifying activity. It has been shown that IFN treatment can disrupt canonical TGF- β signaling and also remodels the BM microvasculature.^{38,39}

In summary, our study showed that expression of mutant JAK2 increases the proportion of CD41^{hi} HSCs that are less robust in maintaining long-term hematopoiesis. IFN- α further accentuated this shift toward CD41^{hi} HSCs, suggesting that continuous conversion of CD41^{lo} to the CD41^{hi} HSC subset may be a mechanism of how IFN- α preferentially targets and exhausts the JAK2 mutant clone.

Acknowledgments

The authors thank members of their laboratory for helpful discussions and critical reading of the manuscript; Albert Neutzner for help with the pegylation of IFN α ; Jean-Luc Villeval for providing the *Jak2-V617F* knock-in mice; Philippe Demougin and Katja Eschbach (D-BSSE, Genomics Facility Basel) for conducting next-generation sequencing; sciCORE (<http://scicore.unibas.ch/>) Scientific Computing Center at the University of Basel for performing analyses of RNASeq data; and Kristina Pannen for help with shipment of samples.

This work was supported by grants from the Swiss National Science Foundation (31003A-147016/1, 31003A_166613, and 31003A_179490), SystemsX.ch (Medical Research and Development grant 2014/266), the Swiss Cancer League (KFS-3655-02-2015 and KFS-4462-02-2018) (R.C.S.), the German Research Foundation (DFG KO 2155/6-1) (S.K.), and by the Czech Science Foundation grant 17-05988S (J.S.).

Authorship

Contribution: T.N.R. designed and performed the research, analyzed the data, and wrote the manuscript; N.H., J.S., D.L.P., J.H., M.E., N.A., L.K., M.R., H.H.-S., C.B., and S.D. performed the research and analyzed the data; F.G., M.K., T.S., T.H.B., D.W., and S.K. analyzed the data; and R.C.S. designed the research, analyzed the data, and wrote the manuscript.

Conflict-of-interest disclosure: R.C.S. has consulted for and received honoraria from Novartis, Shire, and Baxalta. S.K. reports research funding from Novartis, AOP Orphan Pharmaceuticals AG, and Bristol-Myers

Squibb as well as consultancy honoraria and travel reimbursements from Novartis, AOP Orphan Pharmaceuticals AG, and Bristol-Myers Squibb. DW consulted for and received honoraria from Novartis, BMS/Celgene and Baxalta. T.H.B. has consulted for and/or received honoraria from Pfizer Novartis, Ariad and Janssen and research support from Novartis and Pfizer. The remaining authors declare no competing financial interests.

The current affiliation for T.N.R. is Department of Hematology and Central Hematology Laboratory, Inselspital, Bern University Hospital, University of Bern and Department for BioMedical Research, University of Bern, Bern, Switzerland.

ORCID profiles: J.S., 0000-0003-4301-2856; T.S., 0000-0001-9320-0252; T.H.B., 0000-0002-9677-3723; S.K., 0000-0002-1011-8171.

Correspondence: Radek C. Skoda, Department of Biomedicine, University of Basel—University Hospital Basel, Hebelstrasse 20, 4031 Basel, Switzerland; e-mail: radek.skoda@unibas.ch; and Tata Nageswara Rao, Department of Hematology and Central Hematology Laboratory, Inselspital, Bern University Hospital, University of Bern and Department for BioMedical Research, University of Bern, Murtenstrasse 40, 3008 Bern, Switzerland; e-mail: tata.nageswararao@dbmr.unibe.ch.

Footnotes

Submitted 28 February 2020; accepted 8 February 2021; prepublished online on *Blood* First Edition 24 February 2021. DOI 10.1182/blood.2020005563.

The RNA-sequencing data have been submitted to the Gene Expression Omnibus under accession number GSE132570 and GSE 116571.

For original data and reagents, please contact radek.skoda@unibas.ch.

The online version of this article contains a data supplement.

There is a *Blood* Commentary on this article in this issue.

The publication costs of this article were defrayed in part by page charge payment. Therefore, and solely to indicate this fact, this article is hereby marked "advertisement" in accordance with 18 USC section 1734.

REFERENCES

1. Yamamoto R, Morita Y, Ooehara J, et al. Clonal analysis unveils self-renewing lineage-restricted progenitors generated directly from hematopoietic stem cells. *Cell*. 2013;154(5):1112-1126.
2. Sanjuan-Pla A, Macaulay IC, Jensen CT, et al. Platelet-biased stem cells reside at the apex of the haematopoietic stem-cell hierarchy. *Nature*. 2013;502(7470):232-236.
3. Gekas C, Graf T. CD41 expression marks myeloid-biased adult hematopoietic stem cells and increases with age. *Blood*. 2013;121(22):4463-4472.
4. Haas S, Hansson J, Klimmeck D, et al. Inflammation-Induced Emergency Megakaryopoiesis Driven by Hematopoietic Stem Cell-like Megakaryocyte Progenitors. *Cell Stem Cell*. 2015;17(4):422-434.
5. Nishikii H, Kanazawa Y, Umamoto T, et al. Unipotent Megakaryopoietic Pathway Bridging Hematopoietic Stem Cells and Mature Megakaryocytes. *Stem Cells*. 2015;33(7):2196-2207.
6. Rodriguez-Fraticelli AE, Wolock SL, Weinreb CS, et al. Clonal analysis of lineage fate in native haematopoiesis. *Nature*. 2018;553(7687):212-216.
7. Shin JY, Hu W, Naramura M, Park CY. High c-Kit expression identifies hematopoietic stem cells with impaired self-renewal and megakaryocytic bias. *J Exp Med*. 2014;211(2):217-231.
8. Grinenko T, Arndt K, Portz M, et al. Clonal expansion capacity defines two consecutive developmental stages of long-term hematopoietic stem cells. *J Exp Med*. 2014;211(2):209-215.
9. Kent DG, Copley MR, Benz C, et al. Prospective isolation and molecular characterization of hematopoietic stem cells with durable self-renewal potential. *Blood*. 2009;113(25):6342-6350.
10. Gur-Cohen S, Itkin T, Chakrabarty S, et al. PAR1 signaling regulates the retention and recruitment of EPCR-expressing bone marrow hematopoietic stem cells [published correction appears in *Nat Med*. 2016 Apr;22(4):446]. *Nat Med*. 2015;21(11):1307-1317.
11. Vainchenker W, Kralovics R. Genetic basis and molecular pathophysiology of classical myeloproliferative neoplasms. *Blood*. 2017;129(6):667-679.
12. Arber DA, Orazi A, Hasserjian R, et al. The 2016 revision to the World Health Organization classification of myeloid neoplasms and acute leukemia. *Blood*. 2016;127(20):2391-2405.
13. Bellosillo B, Martínez-Avilés L, Gimeno E, et al. A higher JAK2 V617F-mutated clone is observed in platelets than in granulocytes from essential thrombocythemia patients, but not in patients with polycythemia vera and primary myelofibrosis. *Leukemia*. 2007;21(6):1331-1332.
14. Li S, Kralovics R, De Libero G, Theodorides A, Gisslinger H, Skoda RC. Clonal heterogeneity in polycythemia vera patients with JAK2 exon12 and JAK2-V617F mutations. *Blood*. 2008;111(7):3863-3866.
15. Lundberg P, Takizawa H, Kubovcakova L, et al. Myeloproliferative neoplasms can be initiated from a single hematopoietic stem cell expressing JAK2-V617F. *J Exp Med*. 2014;211(11):2213-2230.

16. Kiladjan JJ. Long-term treatment with interferon alfa for myeloproliferative neoplasms. *Lancet Haematol.* 2017;4(4):e150-e151.
17. Essers MA, Offner S, Blanco-Bose WE, et al. IFN α activates dormant haematopoietic stem cells in vivo. *Nature.* 2009;458(7240):904-908.
18. Tiedt R, Hao-Shen H, Sobas MA, et al. Ratio of mutant JAK2-V617F to wild-type Jak2 determines the MPD phenotypes in transgenic mice. *Blood.* 2008;111(8):3931-3940.
19. Hasan S, Lacout C, Marty C, et al. JAK2V617F expression in mice amplifies early hematopoietic cells and gives them a competitive advantage that is hampered by IFN α . *Blood.* 2013;122(8):1464-1477.
20. Grisouard J, Li S, Kubovcakova L, et al. JAK2 exon 12 mutant mice display isolated erythrocytosis and changes in iron metabolism favoring increased erythropoiesis. *Blood.* 2016;128(6):839-851.
21. Schaefer BC, Schaefer ML, Kappler JW, Marrack P, Kedl RM. Observation of antigen-dependent CD8+ T-cell/ dendritic cell interactions in vivo. *Cell Immunol.* 2001;214(2):110-122.
22. Müller U, Steinhoff U, Reis LF, et al. Functional role of type I and type II interferons in antiviral defense. *Science.* 1994;264(5167):1918-1921.
23. Mansier O, Kilani B, Guitart AV, et al. Description of a knock-in mouse model of JAK2V617F MPN emerging from a minority of mutated hematopoietic stem cells. *Blood.* 2019;134(26):2383-2387.
24. Rodgers JT, King KY, Brett JO, et al. mTORC1 controls the adaptive transition of quiescent stem cells from G0 to G(Alert). *Nature.* 2014;510(7505):393-396.
25. Baldridge MT, King KY, Boles NC, Weksberg DC, Goodell MA. Quiescent haematopoietic stem cells are activated by IFN-gamma in response to chronic infection. *Nature.* 2010;465(7299):793-797.
26. Pietras EM, Lakshminarasimhan R, Techner JM, et al. Re-entry into quiescence protects hematopoietic stem cells from the killing effect of chronic exposure to type I interferons. *J Exp Med.* 2014;211(2):245-262.
27. Mullally A, Bruedigam C, Poveromo L, et al. Depletion of Jak2V617F myeloproliferative neoplasm-propagating stem cells by interferon- α in a murine model of polycythemia vera. *Blood.* 2013;121(18):3692-3702.
28. Dumont FJ, Coker LZ. Interferon-alpha/beta enhances the expression of Ly-6 antigens on T cells in vivo and in vitro. *Eur J Immunol.* 1986;16(7):735-740.
29. Yokota T, Oritani K, Butz S, et al. The endothelial antigen ESAM marks primitive hematopoietic progenitors throughout life in mice. *Blood.* 2009;113(13):2914-2923.
30. Ooi AG, Karsunky H, Majeti R, et al. The adhesion molecule esam1 is a novel hematopoietic stem cell marker. *Stem Cells.* 2009;27(3):653-661.
31. Zheng L, Li MP, Gou ZP, et al. A pharmacokinetic and pharmacodynamic comparison of a novel pegylated recombinant consensus interferon- α variant with peginterferon- α -2a in healthy subjects. *Br J Clin Pharmacol.* 2015;79(4):650-659.
32. Nakamura-Ishizu A, Matsumura T, Stumpf PS, et al. Thrombopoietin Metabolically Primes Hematopoietic Stem Cells to Megakaryocyte Lineage Differentiation. *Cell Rep.* 2018;25(7):1772-1785 e1776.
33. Rao TN, Hansen N, Hilfiker J, et al. JAK2-mutant hematopoietic cells display metabolic alterations that can be targeted to treat myeloproliferative neoplasms. *Blood.* 2019;134(21):1832-1846.
34. Baumeister J, Chatain N, Hubrich A, et al. Hypoxia-inducible factor 1 (HIF-1) is a new therapeutic target in JAK2V617F-positive myeloproliferative neoplasms. *Leukemia.* 2020;34(4):1062-1074.
35. Roch A, Trachsel V, Lutolf MP. Brief Report: Single-Cell Analysis Reveals Cell Division-Independent Emergence of Megakaryocytes From Phenotypic Hematopoietic Stem Cells. *Stem Cells.* 2015;33(10):3152-3157.
36. Walter D, Lier A, Geiselhart A, et al. Exit from dormancy provokes DNA-damage-induced attrition in hematopoietic stem cells. *Nature.* 2015;520(7548):549-552.
37. Austin RJ, Straube J, Bruedigam C, et al. Distinct effects of ruxolitinib and interferon-alpha on murine JAK2V617F myeloproliferative neoplasm hematopoietic stem cell populations. *Leukemia.* 2020;34(4):1075-1089.
38. Ulloa L, Doody J, Massagué J. Inhibition of transforming growth factor-beta/SMAD signalling by the interferon-gamma/STAT pathway. *Nature.* 1999;397(6721):710-713.
39. Prendergast AM, Kuck A, van Essen M, Haas S, Blaszkiewicz S, Essers MA. IFN α -mediated remodeling of endothelial cells in the bone marrow niche. *Haematologica.* 2017;102(3):445-453.